Choice between film or powder of PA11 for processing flax fiber-reinforced composites

Fanny Destaing[1], Patricia Jouannot-Chesney[2], Moussa Gomina[2], Joël Bréard[3]

1. Cetim, 74 route de la Jonelière, F-44308 Nantes Cedex 3, France

2. Crismat, UMR 6508 CNRS, ENSICAEN
 6 Boulevard Maréchal Juin, F-14050 Caen Cedex 4, France
 moussa.gomina@ensicaen.fr

3. LOMC, UMR 6294 CNRS, Université du Havre
 53 rue Prony, BP540, 76058 Le Havre, France

ABSTRACT. The biosourced Polyamide 11 (PA11) is envisaged as a matrix in structural eco-composites in combination with long flax fibers. Herein we compare the thermal, rheological, physical, mechanical and hydrothermal behavior of PA11 available as film or powder. These data are used for choosing between the two forms of the PA11 and to determine the temperature, holding time and pressure ranges suited for the elaboration of biocomposites by induction heating.

RÉSUMÉ. Le polyamide 11 (PA11) biosourcé est envisagé comme matrice d'éco-composites structuraux en association avec des fibres longues de lin. Ici nous comparons les comportements thermiques, rhéologiques, physiques, mécaniques et hygrothermiques de deux types de PA11 (sous forme de film ou de poudre). Ces données sont utiles pour choisir sous quelle forme il faudra utiliser le PA11, et pour déterminer la température, le temps de maintien et les plages de pression convenables pour l'élaboration de composites biosourcés en procédant par un chauffage inductif.

KEYWORDS: PA11 thermoplastic resin, flax fiber, thermal characteristics, physical and mechanical properties, rheology, thermocompression biocomposites, hydrothermal ageing.

MOTS-CLÉS : résine thermoplastique PA11, fibre de lin, caractéristiques thermiques, propriétés physiques et mécaniques, rhéologie, thermocompression, biocomposites, vieillissement hygrothermique.

1. Introduction

During the past two decades, environmental concerns and the depletion of oil-based resources have focused attention on renewable natural resources. In the field of composite materials, the potential of plant fibers is evaluated in order to substitute the synthetic fibers derived from petroleum resources. This led in a first step to the development of biocomposites combining short plant fibers and thermosetting resins derived from oil route. Efforts now focus on composites combining long plant fibers with thermoplastic resins for applications in various fields including automotive, sports, furniture, etc. The use of biosourced resins is due to the concern for the recycling of these materials at the end of life.

With this in mind, we seek to develop a composite material with high hydric and mechanical performance from long flax fibers and a biosourced Polyamide 11 (PA11) resin developed for various applications such as fuel or cooling fluid lines, packaging, electrical and electronic equipment, etc. Since the implementation conditions of PA11 determine the quality of the matrix of the composite, this study is undertaken to afford a guideline for the choice of the form of PA11 to be used (powder or film).

2. Materials and Methods

2.1. Bio-based PA11

PA11 is a bio-based polymer obtained from castor oil, a vegetable of euphorbiaceae group mainly cultivated in China, India and Brazil. PA11 is a thermoplastic polymer of the family of aliphatic polyamides prepared by polycondensation of amino acids (Kohan et al., 2003). It is often known as Rilsan[®] B or nylon 11 and has been produced since 1950 by Arkema (CERDATO plant at Serquigny, France).

This thermoplastic polymer is used in a large range of applications: automotive (hydraulic clutch, pneumatic circuits…), oil and gas industry (pipes and fittings for gas), food industry (food films for packaging), sport and leisure (skis, football and cycling shoes...), sterilizable medical equipment (elements of syringes and catheters...), weapons, pipes of mean and high pressure flow of industrial fluids and fuel.

2.2. Characterization methods

Two grades of PA11 were provided by Arkema: extruded films of Rilsan[®] PA11 Besno TL with thickness 150, 200 and 250 µm; and Rilsan[®] PA11 T7500 powder (obtained from cryogenically ground granules about 200 µm in diameter). The chemical structure of PA11 can be described by a sequence of 10 nonpolar methylene units (-CH2-) surrounded by the amide (NH) and C = O groups (Capsal, 2008). The high rate of hydrogen bonds between adjacent chains explains the great

cohesion of the crystalline framework. The lattice is triclinic with parallel arrangement of the chains. Different methods were implemented to characterize the PA11:

– Thermogravimetric analysis (TGA) was performed to determine the onset of the degradation temperature of PA11. This value is regarded as the upper limit of the temperature suitable for the implementation of the composite. The tests were run using thermoformed films of PA11 in a Perkin Elmer TGA 7 apparatus under 80 mL/min nitrogen flow at a heating rate of 20°C/min.

– Differential scanning calorimetry (DSC) tests were performed with Perkin Elmer DSC 4000 type apparatus using sealed aluminum capsules as crucibles.

– Differential thermomechanical analyses (DTMA) were implemented in the torsion mode and controlled stress (5.1 Pa) at a frequency of 1 Hz in the temperature range 190°C – 230°C. Data acquisition was made in increments of 2.5°C and 5s break between two successive measurements. The measuring conditions were selected so that the behavior of the material obeys the laws of linear viscoelasticity.

– Rheological analyses were performed to define the best compromise between PA11 with low viscosity (necessary for a good impregnation of the fibrous reinforcement) and early onset of degradation of the polymer (due to a too long exposure at high temperature). Experiments were conducted on a TA Instrument device (RA 1000) with parallel-plate fixtures using plates of diameter 25 mm and a gap of 3 mm to record the evolution of the viscosity versus temperature and to investigate the stability of the polymer as a function of time and temperature.

– Hydrothermal ageing was implemented on identical PA11 specimens with rectangular section immersed in a thermostatic bath of demineralized water. At different dates a sample is taken and dried on tissue paper before being weighed for moisture content evaluation.

– Physical and mechanical properties of PA11 have been investigated using samples obtained by thermocompression at 200°C under 3 MPa. Slices 15 μm thick cut using Leica RM2155 type ultramicrotome were observed using a polarizing microscope equipped with LAS Core software.

– Scanning Electron Microscopy (SEM) was implemented using Philips FEG type apparatus to analyze the failure mechanisms.

– Hydrothermal behavior of PA11 obtained from powder was assessed by running displacement-controlled tensile tests according to NF ISO 527-1 standard, with the aim to check the influence of the temperature in the range -20°C – +40°C, i.e. well below the glass transition temperature.

3. Results and discussion

3.1. Thermogravimetric analyses

Results show that the thermal instability of PA11 occurs in the temperature range 350°C – 730°C with two detectable peaks. The more pronounced peak occurs

between 400°C and 530°C as was noted by Capsal (*2008*). It is assigned to the degradation of the carbon chain. The secondary peak not observed by Capsal, extends up to 730°C and could be due to the degradation of the double bond connecting the carbon chain and the oxygen atoms. As the degradation of the PA11 begins at around 350°C, one should avoid exposing it to above this temperature during the implementation of the composite, in order to maintain a safety margin.

3.2. Differential scanning calorimetry

The DSC curve of PA11 powder heated up from 0°C to 230°C at a rate of 10°C/min (curve #1 in figure 1) shows an asymmetric melting peak at 186°C. The melting temperature is reported in the literature to be between 182°C and 200°C (Kohan *et al.*, 2003; Jacques *et al.*, 2002; Van Krevelen and Te Nijenhuis, 2009). After cooling from 230°C to 20°C at a rate of 30°C/min, a second heating run up to 230°C at 10°C/min exhibits two distinct endothermic peaks at 180°C and 188°C (curve #2 in figure 1). According to Gaudefroy *et al.* (2002) the peak at 188°C is associated with the melting of a smectic phase whereas the smaller peak occurring at 180°C could be assigned to the melting of a pseudo hexagonal phase. These results point out a polymorphic behavior of the PA11 as a consequence of a relatively slow cooling following the hot pressing. The glass transition temperature of the PA11 determined by DSC is at about 54°C while by DTMA it is evaluated at 58°C. The crystallinity of the PA11, estimated by the ratio of the measured melting enthalpy and the enthalpy of 100% crystalline PA11 (i.e. 189 J/g according to Ricou *et al.*, 2005 or Zhang *et al.*, 2000)) is 41%. The lower crystallinity (25%) associated with the second heating run can be explained by the high cooling rate which does not allow the full development of the crystalline phase in the temperature range between 160°C and 130°C. In figure 1 the behaviors described above are compared with those of the PA11 in two special conditions:

– Curve #3: Using PA11 powder, a thermocompression cycle was simulated in the DSC apparatus as follows: temperature raise from 20°C up to 190°C (assumed maximum temperature the flax fibers can withstand without degradation) at a heating rate of about 100°C/min followed by a dwell of 1 min (corresponding to the impregnation step of the fibers) and then cooling down to 20°C at a rate of 50°C/min (average cooling rate when water-cooling between 190°C and the end of crystallization at about 130°C). After this cycle, the DSC curve recorded from 20°C up to 230°C with a heating rate of 10°C/min exhibits only the endothermic peak (at 190°C) associated with the presence of the smectic phase of PA11;

– Curve #4: Starting from a film of PA11, thermocompression was implemented at 3 MPa while heating by using an induction heating device (RocTool®) from 20°C up to 190°C at a rate of 200°C/min. Then, after a dwell of 1 min, water-cooling is performed at a rate of about 40°C/min. The DSC curve shows only one melting peak at 192°C like the powder of PA11 which has undergone rapid cooling (curve #3). If the film is heated up to 230°C at a rate of 10°C/min and then cooled down at 30°C/min, its DSC curve exhibits the two peaks characteristic of polymorphism (curve #5).

Thus, the implementation of the composite must be made at a temperature equal or above 190°C. A rapid cooling rate leads to the existence of only the smectic phase.
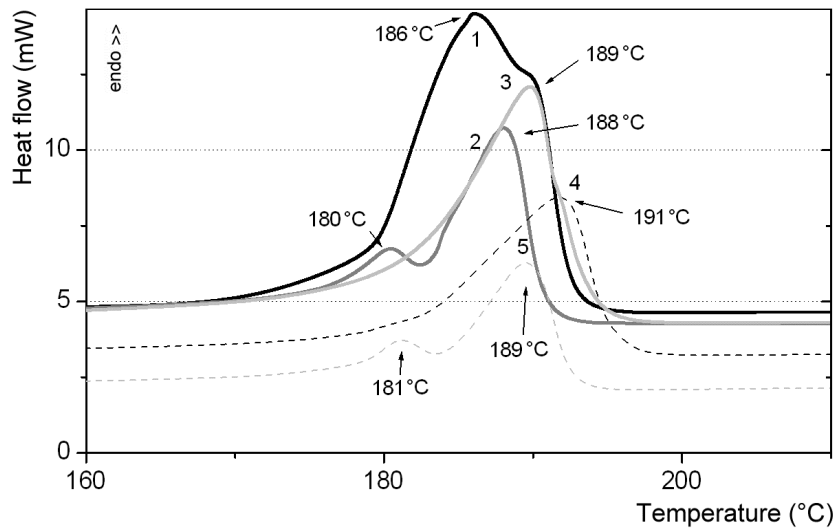

Figure 1. Influence of the heating conditions on the thermal behavior of PA11 obtained from powder or film

3.3. Rheological analyses

The viscosity was determined as a function of time for different temperatures. In the early times, the viscosity of the PA11 at 190°C is almost 20 times higher than at T > 200°C. However at 190°C the viscosity is constant in the explored time interval, which means that the polymer does not degrade. At higher temperatures the viscosity increases almost exponentially for a holding time longer than 200s. This means that the impregnation of the fibers by the PA11 will no longer be possible. The increase in viscosity is certainly related to an increase in the molecular weight (M_w), or even polymer degradation. Thus, the implementation of the composite should be made on short time at a temperature above 190°C.

To refine these operating conditions, the change of viscosity as a function of the temperature at different times was investigated (figure 2). This figure shows that the increase in temperature allows obtaining a more liquid PA11 at low exposure time (< 300 s). Indeed, if the PA11 is exposed above 200°C for longer than 300s, crosslinking continues and the polymer becomes more viscous with time. Therefore, composite implementation beyond 210°C must be avoided if the cycle lasts more than 5 minutes.
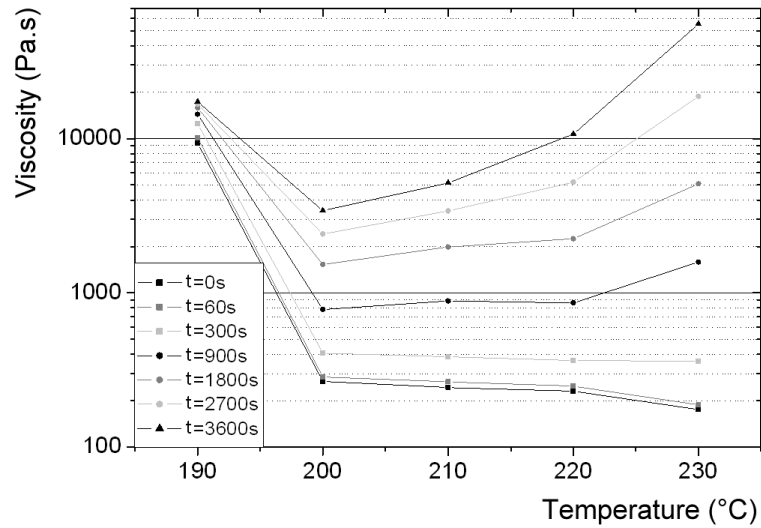
Figure 2. Viscosity change versus temperature for different holding times
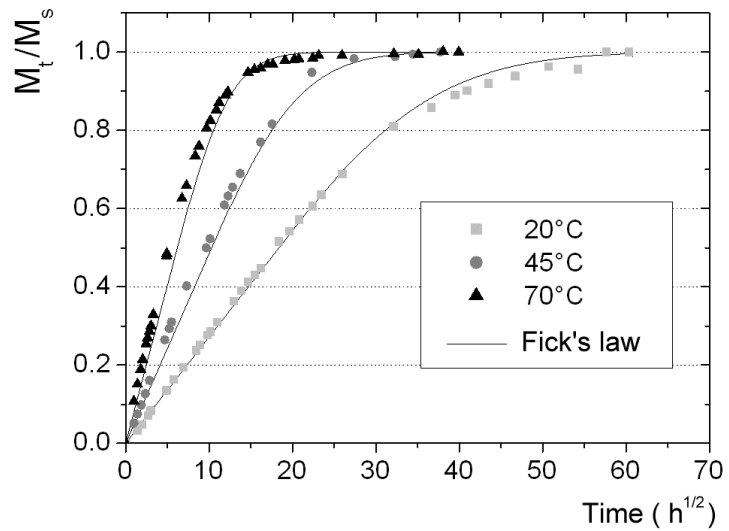

*Figure 3. Weight evolution as a function of $t^{1/2}$ relatively to the saturation level
for different temperatures, and comparison to the one dimension Fickian law*

3.4. Hydrothermal ageing

Water ageing of polymer matrix composites occurs via the matrix as the synthetic reinforcement (glass or carbon fibers) may be considered inert. However, in the case of plant fiber-reinforced composites, water can also degrade the fiber *via* the weakly bonded fiber/matrix interface and singularities in the fiber like the lumen or induced defects in the decortication stage (Thuault *et al.*, 2014). Figure 3 shows the relative evolution of the samples' mass, M_t, versus the square root of the immersion time, $t^{1/2}$, for three bath temperatures, according to the Fickian diffusion model. The linear shape of the curves and their overlap for different thicknesses of test specimens in the range of low immersion time testify that the hydric behavior of PA11 is well described by Fick's law. Aliphatic polyamides are highly hydrophilic, the maximum amount of water absorbed under relative humidity of 100% being proportional to the density of amide groups (Starkweather *et al.*, 1956). Maximum hydration rate of 1.5% was reported for PA11 (Takase *et al.*, 1991; Bos *et al.*, 2004; Newman *et al.*, 1990) although the level may vary depending on the immersion temperature.

The incidence of hydrothermal ageing on the viscoelastic behavior of PA11 was studied by DTMA (see the paragraph above). The DMTA highlights two of the three types of solid transition of the PA11 (the melting zone cannot be measured with this type of analysis) as it is performed on a solid material. The glass transition temperature is evaluated at 58°C. Figure 4a shows the change in the viscoelastic behavior of the PA11 versus the water content. The area under the transition peak is unchanged but the maximum of the peak is shifted toward the low temperatures. This shift is characteristic of plasticization of the polymer by inclusion of water molecules between the secondary bonds in the amorphous phase, which contributes to increase chain mobility. As can be seen in figure 4a, the Tg decreases by 15°C for water uptake of 0.5% (in the first 250 hours of holding stage). When the water content is increased, the Tg remains constant. This feature had been reported by Poulard (1998). The glass transition temperature is very sensitive to the presence of water, but almost not in its content. It is also noted that the peak width increases with the water content. This could be due to the cleavage of the macromolecular chains by the unbound water that is inserted between them. Indeed, peak broadening is due to the increase in chain lengths distribution (Risson, 1998), the shortest chains having a lower relaxation temperature. Moreover, when drying a sample saturated with water, it recovers the initial mass. This means that the water saturation entails neither leaching (chemical ageing) nor hydrolysis of the PA11.

In figure 4b the effect of water uptake on the viscoelastic behavior of the PA11 is evaluated in terms of the change of tan δ curve versus temperature. A dried sample is first saturated with water at 20°C and then progressively dried and the mass is measured regularly during the drying. We noticed that the curve at saturation is not only shifted toward the low temperatures, but its shape changes significantly: it is broader, less symmetric and the maximum is lowered. The shape of the peak becomes exactly the same as before ageing but with a lower maximum; Tg returns to its original value. From these observations, it is concluded that the hydrothermal

ageing of PA11 at 20°C is reversible. Water only affects the physical properties of the polymer; the only mechanism activated is plasticization (physical ageing).
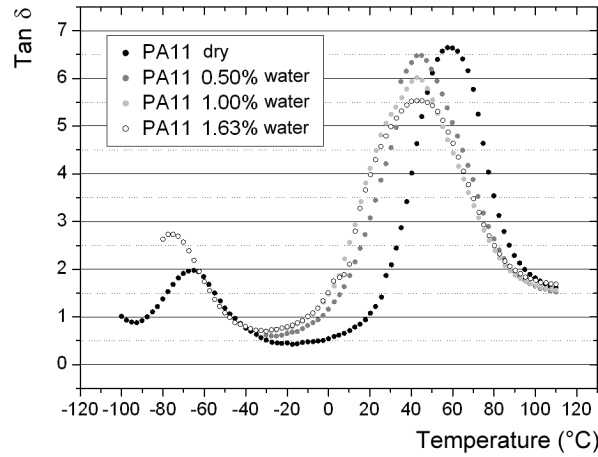

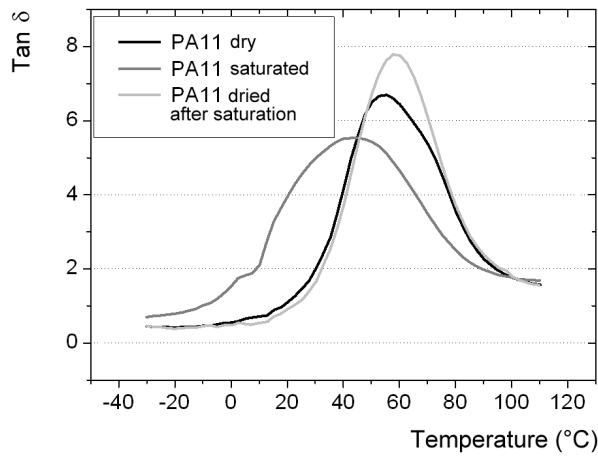*Figure 4a. Evolution of tanδ versus temperature for different water contents*

Figure 4b. Influence of drying on tanδ without or after water saturation

3.5. Microstructure observation

The microstructure shown in figure 5a reveals the presence of spherulites in the material obtained from powder while that developed from film does not contain any (figure 5b), although it is also crystalline. Spherulites in figure 5a are very similar to those observed by Lefebvre (2002), but other types of spherulites were reported (Landreau, 2008).
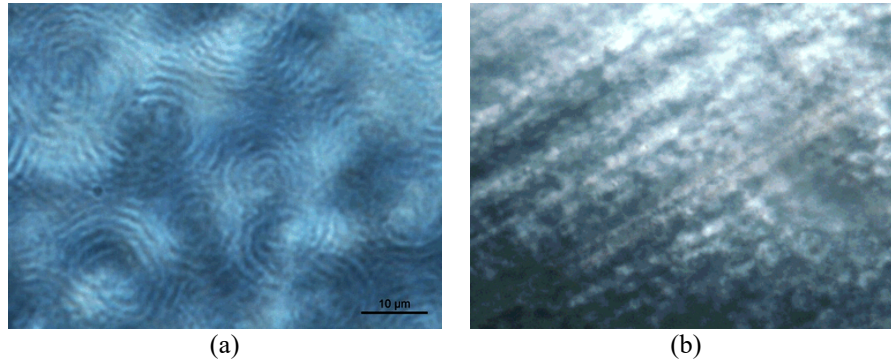
<center>(a)</center> <center>(b)</center>

Figure 5. Polarized light micrographs of PA11 obtained from powder (a) or film (b)
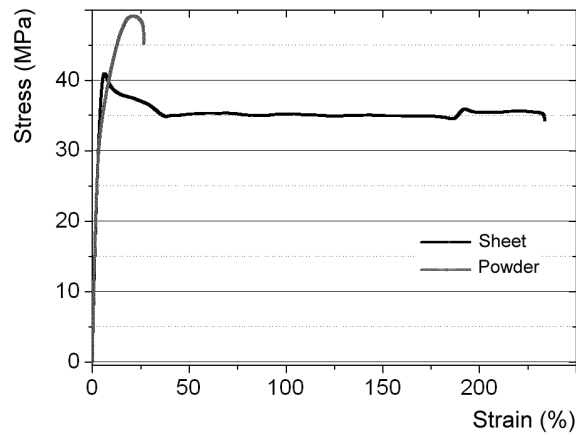

Figure 6. Tensile loading curves of PA11 obtained from powder or film

3.6. Hydrothermal behavior and mechanical properties

3.6.1. Unaged materials

3.6.1.1. Loading curves at room temperature

The uniaxial tensile stress-strain curves of the materials made from powder or film (dumbbell specimens with gauge length 70 mm, width 10 mm and loaded at a displacement rate of 1 mm/min at 20°C and RH = 60%) behave totally different (figure 6). The loading curve of PA11 obtained from films exhibits a characteristic shape of a semi-crystalline thermoplastic polymer with a quasi-plastic behavior prior to rupture at an ultimate deformation of about 225%. The estimated elastic modulus is approximately 1.5 GPa, with a macroscopic plastic flow threshold at ($\sigma_y = 41$ MPa and $\varepsilon_y = 3\%$). The material obtained from powder is much less deformable, with an

ultimate strain of about 25%, strength of about 50 MPa and Young's modulus identical to that of PA11 made from films (1.5 GPa). This behavior is assigned to the spherulitic crystalline structure that hinders the necking and thus the high elongation.
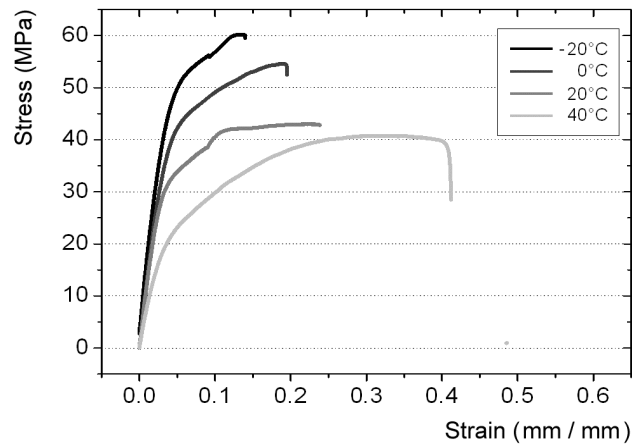

Figure 7. Tensile loading curves of PA11 obtained from powder vs. temperature
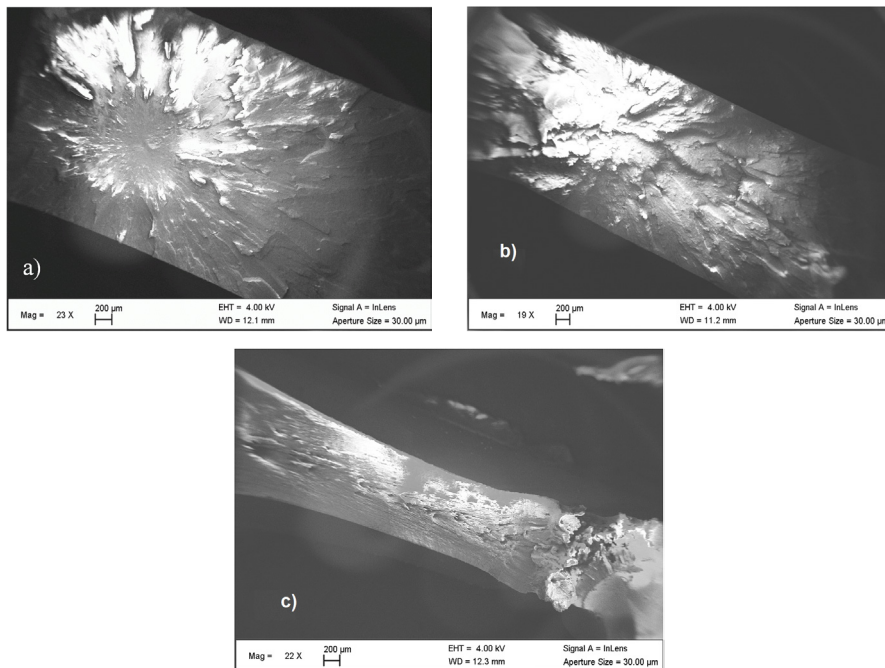

Figure 8. Fracture surfaces of tensile loaded PA11 obtained from powder vs. temperature: up to 0°C (a); 20°C (b) and 40°C (c)

3.6.1.2. Mechanical behavior vs. temperature for PA11 obtained from powder

Overall, up to 0°C the brittle behavior reported in figure 7 correlates with a smooth surface of rupture around the critical defect (figure 8a). At 20°C failure occurs at around ε_R=15% before necking. The highly disordered fracture surfaces makes indiscernible the critical defect (figure 8b); a mixed brittle/ductile behavior is observed. At 40°C the ductile behavior is very marked with an ultimate strain of about 40% (figure 8c).

3.6.2. Water-aged material

3.6.2.1. Mechanical behavior

PA11 obtained from powder was aged in demineralized water at 20°C for 2000 hours. This temperature was selected well below Tg of unaged material (58°C) so that the water intake is not accelerated by the consequent increase in the mobility of the macromolecules. This material was tensile-loaded at different temperatures (figure 9) in order to estimate the reduction in mechanical properties.

The effects of ageing on the mechanical properties of PA11 under different temperatures are discussed below (figures 10a to 10e):

– For unaged PA11, variations of the ultimate deformation, strength, Young's modulus and macroscopic plastic flow stress as a function of test temperature can be described by two distinct zones. The first zone which extends up to 20°C shows a linear variation of the considered parameter vs temperature with a moderate slope. The second zone extends beyond 20°C and shows a higher slope;

– For aged specimens the boundary between the two zones is at 0°C, except for the yield strain (estimated by using the Considere's construction). Paradoxically, until about 20°C the aged PA11 Young's modulus is higher.
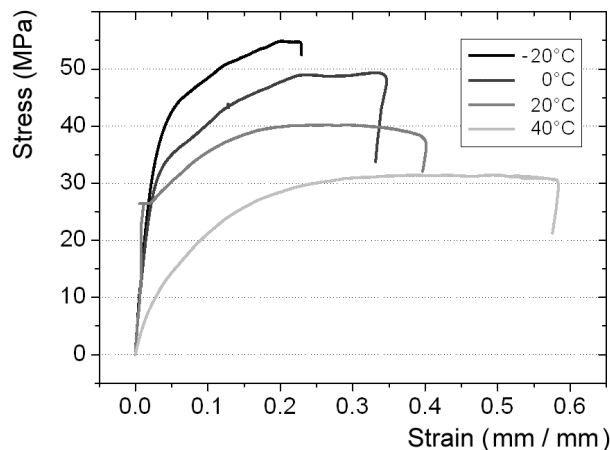

Figure 9. Tensile loading curves of PA11 obtained from powder: influence of temperature after water ageing
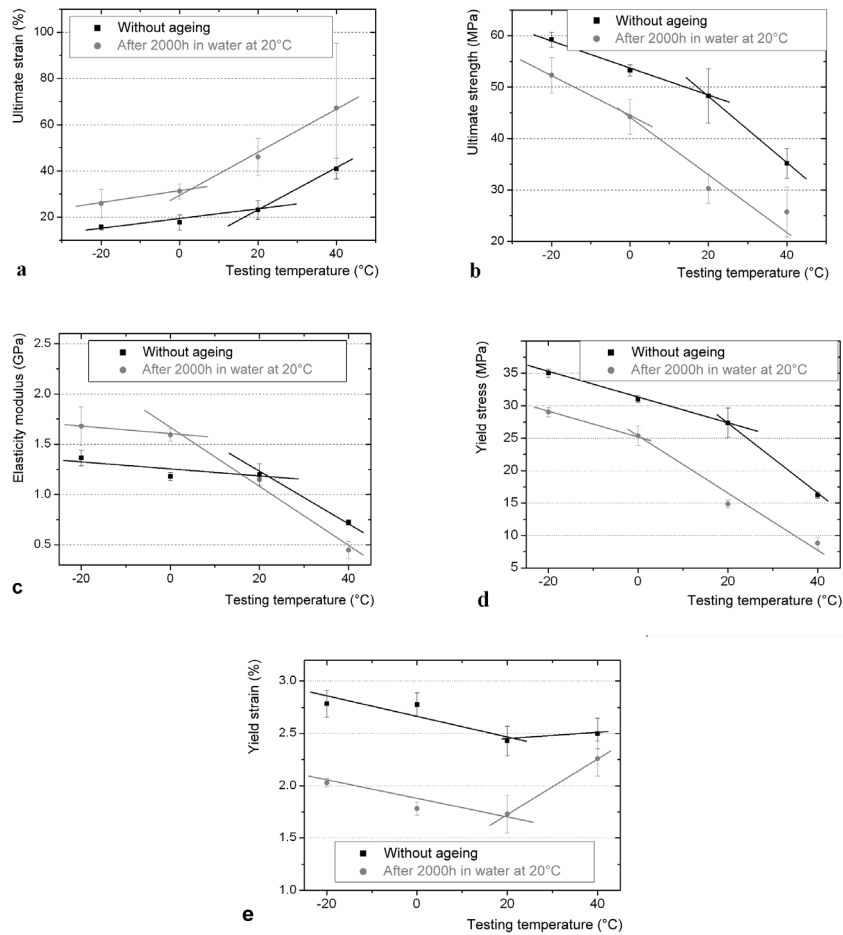
Figure 10. Influence of the temperature and the hydrothermal ageing on the mechanical behavior of PA11 obtained from powder

Referring to the Tg of the unaged PA11 that is approximately 58°C, the hinge temperature at 20°C corresponds to that found at the foot of tanδ curve, i.e. the beginning of the glass transition region. Beyond this temperature, at 40°C for example, is the beginning of the rubbery domain. By contrast, for the aged PA11 with Tg of about 42°C, the hinge temperature at 0°C corresponds to the beginning of the rubbery domain. Below 20°C, the higher Young's modulus for the aged material could be explained by the presence of frozen unbound water. By the low water mobility at low temperatures, the overall stiffness of the material is increased.

3.6.2.2. SEM analysis

The variations of the mechanical parameters versus temperature are correlated with the observations of the fracture surfaces by electronic scanning microscopy (figures 11a to 11d). The observed brittle behavior up to a temperature of -20°C (Fig. 11a) turns to ductile at 0°C (Fig. 11b). Necking becomes important at 20°C but its extension is upset by the tearing of the polymer as evidenced by the cupules (Fig. 11c). At 40°C the necking is more pronounced and the specimen behaves highly ductile. These cupules are rather related to the presence of inclusions type defects. Indeed the phenomenon of osmotic pressure is excluded as water uptake curves do show neither mass recovery (hydrolysis) nor mass loss (leaching).
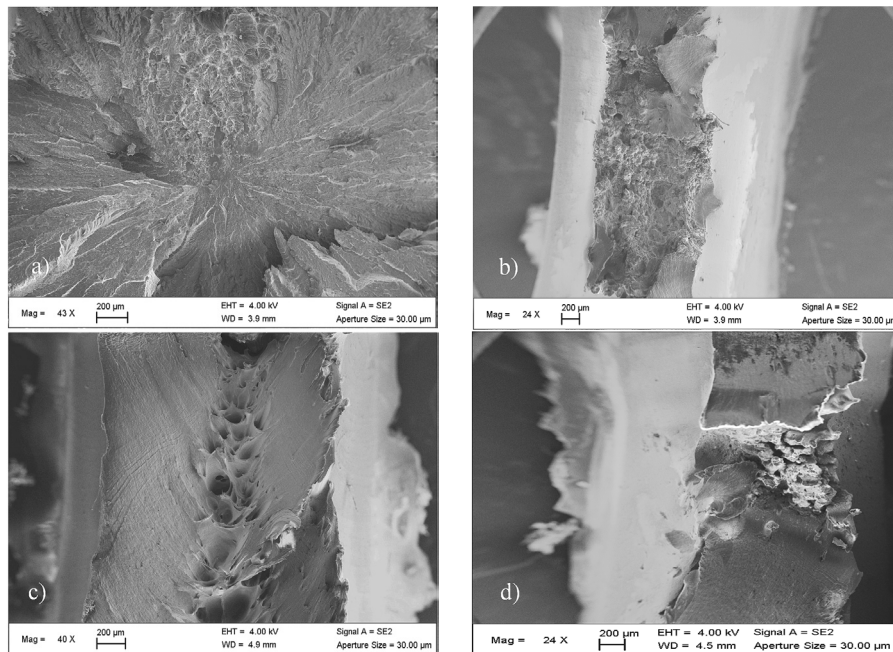
Figure 11. Fracture surfaces of water-aged PA11 specimens tested at different temperatures: -20°C (a); 0°C (b); 20°C (c) and 40°C (d)

4. Conclusion

This study aimed to understand the properties of PA11 for optimizing the implementation parameters of composites incorporating flax fibers. The main findings are summarized below:

– TGA results indicate that the implementation of the composite should be made below 350°C to avoid degradation of the PA11. The DSC study highlights the polymorphism of PA11 according to the cooling rate. At low cooling rates, smectic

phase and pseudo hexagonal phase crystals coexist. When the cooling rate is too high to allow complete and distinct genesis of these two phases, the apparent peak is almost that of the smectic phase which occurs at high temperature. Also, the degree of crystallinity estimated from the enthalpy of fusion is very dependent on the cooling rate. The DSC curves also indicate that PA11 melting temperature is close to 190°C. This implies that the implementation of the composite should be made at a temperature equal or exceeding 190°C.

– Rheological investigations indicate that the viscosity of the PA11 decreases strongly beyond 190°C. However, holding the polymer for over 300s in the temperature range 200°C – 220°C raises the viscosity beyond a level incompatible with a good impregnation of the fibrous preform.

– The glass transition temperature of the dry PA11 is in the range 54° – 58°C, as estimated by DSC or DTMA.

– Hydrothermal ageing of PA11 at 20°C is reversible and occurred by a plasticization mechanism only.

– The water absorption kinetics follows a Fickian law, with a maximum content of 1.7%. At saturation Tg is reduced by about 20°C while the glass transition zone widens significantly; this reduction of Tg is completely recovered after drying.

– Compared with the PA11 obtained by thermocompression of films, PA11 obtained from powder shows a much lower ultimate deformation due to its higher organized crystalline structure, and a higher fluidity at 190°C which is the processing temperature of the flax fiber / PA11 composites.

Thus, the PA11 will be chosen as a powder for the manufacture of biocomposites by thermocompression in combination with flax fiber fabric for structural applications.

References

Bos H.L., Molenveld K., Teunissen W., Van Wingerde A.M. and Van Delft D.R.V. (2004). Compressive behaviour of unidirectional flax fibre reinforced composites. *Journal of Materials Science*, 39 [6], p. 2159-2168.

Capsal J.F. (2008). *Elaboration and analysis of the physical properties of hybrid ferroelectric nanocomposites*, PhD at the CIRIMAT Laboratory UMR 5085, Toulouse, France.

Gaudefroy V., Chocinski L., Gacougnolle J.-L. and Rivière A. (2002). Influence of smectic phase on the mechanical behavior of polyamide 11 in uniaxial tension, *Matériaux 2002*, Nanterre.

Jacques B., Werth M., Merdas I., Thominette F. and Verdu J. (2002). Hydrolytic ageing of Polyamide 11: 1. Hydrolysis kinetics in water. *Polymer*, 43 [24], p. 6439-6447.

Kohan M.I., Mestemacher S.A., Pagilagan R. and Redmond K. (2003). *Polyamides*, Ullmann's Encyclopedia of Industrial Chemistry.

Landreau E. (2008). *Materials from renewable resources. Plasticized starch/compatibilized PA11 mixtures*, PhD of the University of Reims Champagne-Ardennes, France.

Lefebvre X. (2002). *Slow brittle cracking of polyamide 11: creep mechanisms and lifetime*, PhD of the Mine School of Paris, France.

Newman B.A., Kim K.G. and Scheinbeim J.I. (1990). Effect of water content on the piezoelectric properties of nylon 11 and nylon 7. *Journal of Materials Science*, 25 [3], p. 1779-1783.

Poulard F. (1998). *Adhesion of polyamide 11: mechanisms and hygrothermal ageing*, PhD of the Mine School of Paris, France.

Ricou P., Pinel E. and Juhasz N. (2005). Temperature experiments for improved accuracy in the calculation of polyamide 11 crystallinity by x-ray diffraction. *Advances in X-ray Analysis*, 48, p. 170-175.

Risson T. (1998). *Creep behavior of carbon fiber-reinforced composites with epoxy matrices or PEEK*, PhD of Ecole Centrale de Lyon, France.

Starkweather H.W., Moore G.E., Hansen J.E., Roder T.M. and Brooks R.E. (1956). Effect of crystallinity on the properties of nylons. *J. Polym. Sci.*, 21 [98], p. 189-204.

Takase Y., Lee J.W., Scheinbeim J.I. and Newman B.A. (1991). High-temperature characteristics of nylon-11 and nylon-7 piezoelectrics. *Macromolecules*, 24 [25], p. 6644-6652.

Thuault A., Eve S., Blond D., Bréard J. and Gomina M. (2014). Effects of the hygrothermal environment on the mechanical properties of flax fibres. *Journal of Composite Materials*, 48 [14], p. 1699–1707.

Van Krevelen D.W. and Te Nijenhuis K. (2009). *Properties of polymers: their correlation with chemical structure; their numerical estimation and prediction from additive group contributions (4th Edition)*, ISBN: 978-0-08-054819-7, Elsevier Science.

Zhang Q., Mo Z., Liu S. and Zhang H. (2000). Influence of annealing on structure of Nylon 11, *Macromolecules*, 33 [16], p. 5999-6005.